

Error computation in the uniform color-spaces sRGB and CIE L*a*b*

Ioannis Andreadis, Vasilios Vonikakis and Filippos Tsalides

Abstract - This paper reports a study for the computation of error propagation in the sRGB to CIE L*a*b* color-space transformation. First the mathematical equations, which describe errors, are derived and then, experimental studies with a variety of images are carried out. Experimental results, which are confirmed by the extracted mathematical equations, determine ranges of errors, useful in various color image recognition applications. Furthermore, a comparison of these two uniform color-spaces is carried out.

Index Terms - CIE L*a*b*, sRGB, errors

I. INTRODUCTION

The use of color information in digital image processing is constantly increasing in many applications, such as image segmentation, feature extraction and visual information retrieval. Two principal factors are mainly responsible for this. First, color is a powerful descriptor that often simplifies object identification and extraction from a scene. Second, humans can discern thousands of color shades and intensities, compared to about only two dozen gray shades, a factor that is quite important in image analysis.

When an image is to be imported in a digital system, through a camera or a scanning device, the process of digitization itself introduces a considerable amount of variation in the digital representation of the image, contrary to the human vision system. The main reason for this inconvenience is the non-uniformity of the classical RGB color-space. To overcome this, interest has been focused on perceptually uniform color-spaces such as sRGB and CIE L*a*b*.

In this paper, we attempt to ‘track’ the variations of sRGB color images, through the transformation to the CIE L*a*b* color-space, in order to compare the uniformity of these two color-spaces. Appropriate mathematical formulas are extracted in order to describe and confirm the propagation of errors from sRGB to CIE L*a*b*. Experimental results lead to the conclusion, that the transformation reduces the amount of variance,

introduced in the color channels of the sRGB color-space, through the process of digitization.

II. CIE L*a*b* COLOR-SPACE

The CIE L*a*b* color-space was adopted in 1976 by the CIE (Commission Internationale de l’Eclairage). Unlike other color-spaces, which are based on the hardware of a certain device (RGB on cathode ray tubes and CMYK on printing devices), CIE L*a*b* is based on the human vision system [1]. CIE L*a*b* is a uniform color-space, meaning that the Euclidean geometrical difference of two colors in the color-space, equals the perceptual difference of these two colors [2,3,4]. The basic concepts on which the CIE L*a*b* color-space is founded are:

1. Every color is treated as a combination of surface color and illuminant color, which allows the color model to be applied across a wider range of viewing conditions [4].
2. The color-space is defined by three geometrical axes, each one of them representing one of the three basic concepts of human vision (detection of lightness, detection of greenness-redness and detection of blueness-yellowness) [1,2,4].
3. Equality of geometrical and perceptual color difference in human vision system (perceptually uniform)[2,4].
4. Device independent.

A. CIE L*a*b* color coordinates ranges

Unlike the majority of color-spaces, CIE L*a*b* has not a specific shape for the space that it appoints. Particularly, CIE L*a*b* is conceived as an unbounded and continuous three-dimensional space, but the actual location of colors in this space, detectable by the human vision system, does fall roughly within spherical limits, and thus, many describe it as a sphere [4].

CIE L*a*b* color-space is extracted from the XYZ color-space through a non-linear transformation. Consequently, any transition from a source space to CIE L*a*b*, must cross its path with the XYZ space [2]. Fig.1 shows an overview of the CIE L*a*b* including its boundaries. Fig. 2 and Fig. 3 show, in pseudocode form, the transformations sRGB→XYZ and XYZ→CIE L*a*b*, that are used for the transition sRGB→CIE L*a*b* [5,6].

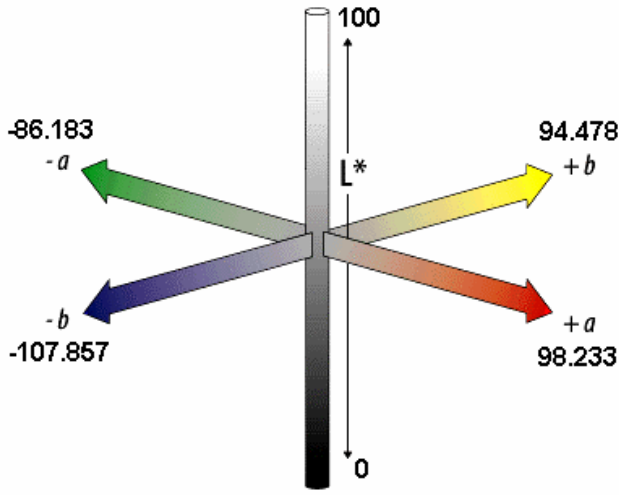


Fig.1 CIE L*a*b* axes with its boundaries

```

var_R = ( digital_R / 255 ) //digital_R= From 0 to 255
var_G = ( digital_G / 255 ) //digital_G= From 0 to 255
var_B = ( digital_B / 255 ) //digital_B = From 0 to 255
if (var_R > 0.03928) var_R = ( ( var_R + 0.055 ) / 1.055 ) ^2.4
else var_R = var_R / 12.92
if (var_G > 0.03928) var_G = ( ( var_G + 0.055 ) / 1.055 )^2.4
else var_G = var_G / 12.92
if (var_B > 0.03928) var_B = ( ( var_B + 0.055 ) / 1.055 )^2.4
else var_B = var_B / 12.92
var_R = var_R * 100
var_G = var_G * 100
var_B = var_B * 100

out_X = var_R * 0.4124 + var_G * 0.3576 + var_B * 0.1805
out_Y = var_R * 0.2126 + var_G * 0.7152 + var_B * 0.0722
out_Z = var_R * 0.0193 + var_G * 0.1192 + var_B * 0.9505

```

Fig.2 The transformation RGB→XYZ

```

ref_X = 95.047 //Observer. = 2°, Illuminant = D65
ref_Y = 100.000
ref_Z = 108.883
var_X = inp_X / ref_X //inp_X = From 0 to ref_X
var_Y = inp_Y / ref_Y //inp_Y = From 0 to ref_Y
var_Z = inp_Z / ref_Z //inp_Z = From 0 to ref_Z
if ( var_X > 0.008856 ) var_X = var_X ^ ( 1/3 )
else var_X = ( 7.787 * var_X ) + ( 16 / 116 )
if ( var_Y > 0.008856 ) var_Y = var_Y ^ ( 1/3 )
else var_Y = ( 7.787 * var_Y ) + ( 16 / 116 )
if ( var_Z > 0.008856 ) var_Z = var_Z ^ ( 1/3 )
else var_Z = ( 7.787 * var_Z ) + ( 16 / 116 )

out_L = ( 116 * var_Y ) - 16
out_a = 500 * ( var_X - var_Y )
out_b = 200 * ( var_Y - var_Z )

```

Fig.3 The transformation XYZ→ CIE L*a*b*

III. SRGB COLOR-SPACE

The increasing need for a perceptually-uniform color-space, that would minimize the perceptual differences between different monitor devices, led Microsoft and Hewlett-Packard to propose the sRGB color-space in 1996. Their proposal was based upon the fact that RGB was the most commonly used color-space and CIE L*a*b* required complex transformations. Consequently, they created a perceptually uniform version of the classical RGB color-space [7,8]. The basic concepts on which sRGB is founded are:

1. The average performance of a typical CRT monitor.
2. Reference viewing conditions.
3. An equal to 2.2 gamma correction to achieve perceptual uniformity.

At the moment, sRGB is widely used in multimedia applications and especially in the Internet.

IV. ERROR COMPUTATION

Let Z be a multivariable function:

$$Z = f(L_1, L_2, \dots, L_k)$$

of random variables, with average values $\bar{L}_1, \bar{L}_2, \dots, \bar{L}_k$.

It is valid to state that [9]:

$$\bar{Z} \approx f(\bar{L}_1, \bar{L}_2, \dots, \bar{L}_k)$$

meaning that 'the value of the function when using the averages of its variables, approximates the average value of the function itself'. In addition, the variance of \bar{Z} can be computed by the following equation [9]:

$$Var(\bar{Z}) \approx \sum_{i=1}^k \left(\frac{\partial \bar{Z}}{\partial L_i} \right)^2 \cdot Var(L_i) + \sum_{i \neq j}^k \sum_{i \neq j}^k \left(\frac{\partial \bar{Z}}{\partial L_i} \right) \left(\frac{\partial \bar{Z}}{\partial L_j} \right) \cdot Cov(L_i, L_j) \quad (1)$$

A. Error Propagation in sRGB→CIE L*a*b*

The transformation sRGB→CIE L*a*b* is actually sRGB→XYZ→CIE L*a*b* [3,5,6]. Consequently, we can express XYZ space as a function of R, G, B, and CIE L*a*b* space as a function of X, Y, Z. As a result of this, since XYZ space is a function of R, G, B, it is possible to express CIE L*a*b* color-space as a function of R, G and B.

$$\left. \begin{aligned} XYZ &= g(R, G, B) \\ CIE L^* a^* b^* &= h(X, Y, Z) \end{aligned} \right\} \Rightarrow CIE L^* a^* b^* = f(R, G, B) \quad (2)$$

Importing R, G, B, to the CIEL*a*b* equations, as equation (2) states, the following three equations, are obtained:

$$L^*(R, G, B) = 24.9914 \left[(R + 14.025)^{2.4} \cdot 3.1334 \cdot 10^{-5} + (G + 14.025)^{2.4} \cdot 1.0542 \cdot 10^{-4} + (B + 14.025)^{2.4} \cdot 1.0642 \cdot 10^{-5} \right]^{\frac{1}{3}} - 16 \quad (3)$$

$$\alpha^*(R, G, B) = 109.561 \left[(R + 14.025)^{2.4} \cdot 6.0787 \cdot 10^{-5} + (G + 14.025)^{2.4} \cdot 5.271 \cdot 10^{-5} + (B + 14.025)^{2.4} \cdot 2.6605 \cdot 10^{-5} \right]^{\frac{1}{3}} - 107.722 \left[(R + 14.025)^{2.4} \cdot 3.1334 \cdot 10^{-5} + (G + 14.025)^{2.4} \cdot 1.0542 \cdot 10^{-4} + (B + 14.025)^{2.4} \cdot 1.0642 \cdot 10^{-5} \right]^{\frac{1}{3}} \quad (4)$$

$$b^*(R, G, B) = 43.0887 \left[(R + 14.025)^{2.4} \cdot 3.1334 \cdot 10^{-5} + (G + 14.025)^{2.4} \cdot 1.0542 \cdot 10^{-4} + (B + 14.025)^{2.4} \cdot 1.0642 \cdot 10^{-5} \right]^{\frac{1}{3}} - 41.8835 \left[(R + 14.025)^{2.4} \cdot 2.8448 \cdot 10^{-6} + (G + 14.025)^{2.4} \cdot 1.757 \cdot 10^{-5} + (B + 14.025)^{2.4} \cdot 1.401 \cdot 10^{-4} \right]^{\frac{1}{3}} \quad (5)$$

Equations (3), (4) & (5), state that L^* , a^* , b^* are functions, of R, G, B, and thus, equation (1) can be used. The approximate calculation of the variances of L^* , a^* , b^* can be obtained as follows:

$$Var(\bar{L}^*) = \left(\frac{\partial \bar{L}^*}{\partial R} \right)^2 VarR + \left(\frac{\partial \bar{L}^*}{\partial G} \right)^2 VarG + \left(\frac{\partial \bar{L}^*}{\partial B} \right)^2 VarB + \left[\frac{\partial \bar{L}^*}{\partial R} \cdot \frac{\partial \bar{L}^*}{\partial G} \cdot Cov(R, G) + \frac{\partial \bar{L}^*}{\partial R} \cdot \frac{\partial \bar{L}^*}{\partial B} \cdot Cov(R, B) + \frac{\partial \bar{L}^*}{\partial G} \cdot \frac{\partial \bar{L}^*}{\partial B} \cdot Cov(G, B) \right] \quad (6)$$

with

$$\frac{\partial \bar{L}^*}{\partial R} = 19.9931 \left[(\bar{R} + 14.025)^{2.4} \cdot 3.1334 \cdot 10^{-5} + (\bar{G} + 14.025)^{2.4} \cdot 1.0542 \cdot 10^{-4} + (\bar{B} + 14.025)^{2.4} \cdot 1.0642 \cdot 10^{-5} \right]^{\frac{2}{3}} \left[(\bar{R} + 14.025)^{1.4} \cdot 3.1334 \cdot 10^{-5} \right] \quad (7)$$

$$\frac{\partial \bar{L}^*}{\partial G} = 19.9931 \left[(\bar{R} + 14.025)^{2.4} \cdot 3.1334 \cdot 10^{-5} + (\bar{G} + 14.025)^{2.4} \cdot 1.0542 \cdot 10^{-4} + (\bar{B} + 14.025)^{2.4} \cdot 1.0642 \cdot 10^{-5} \right]^{\frac{2}{3}} \left[(\bar{G} + 14.025)^{1.4} \cdot 1.0542 \cdot 10^{-4} \right] \quad (8)$$

$$\frac{\partial \bar{L}^*}{\partial B} = 19.9931 \left[(\bar{R} + 14.025)^{2.4} \cdot 3.1334 \cdot 10^{-5} + (\bar{G} + 14.025)^{2.4} \cdot 1.0542 \cdot 10^{-4} + (\bar{B} + 14.025)^{2.4} \cdot 1.0642 \cdot 10^{-5} \right]^{\frac{2}{3}} \left[(\bar{B} + 14.025)^{1.4} \cdot 1.0642 \cdot 10^{-5} \right] \quad (9)$$

$$Var(\bar{\alpha}^*) = \left(\frac{\partial \bar{\alpha}^*}{\partial R} \right)^2 VarR + \left(\frac{\partial \bar{\alpha}^*}{\partial G} \right)^2 VarG + \left(\frac{\partial \bar{\alpha}^*}{\partial B} \right)^2 VarB + \left[\frac{\partial \bar{\alpha}^*}{\partial R} \cdot \frac{\partial \bar{\alpha}^*}{\partial G} \cdot Cov(R, G) + \frac{\partial \bar{\alpha}^*}{\partial R} \cdot \frac{\partial \bar{\alpha}^*}{\partial B} \cdot Cov(R, B) + \frac{\partial \bar{\alpha}^*}{\partial G} \cdot \frac{\partial \bar{\alpha}^*}{\partial B} \cdot Cov(G, B) \right] \quad (10)$$

with

$$\frac{\partial \bar{\alpha}^*}{\partial R} = 5.3279 \cdot 10^{-3} \left[(\bar{R} + 14.025)^{2.4} \cdot 6.0787 \cdot 10^{-5} + (\bar{G} + 14.025)^{2.4} \cdot 5.271 \cdot 10^{-5} + (\bar{B} + 14.025)^{2.4} \cdot 2.6605 \cdot 10^{-5} \right]^{\frac{2}{3}} (\bar{R} + 14.025)^{1.4} - 2.7 \cdot 10^{-3} \left[(\bar{R} + 14.025)^{2.4} \cdot 3.1334 \cdot 10^{-5} + (\bar{G} + 14.025)^{2.4} \cdot 1.0542 \cdot 10^{-4} + (\bar{B} + 14.025)^{2.4} \cdot 1.0642 \cdot 10^{-5} \right]^{\frac{2}{3}} (\bar{R} + 14.025)^{1.4} \quad (11)$$

$$\frac{\partial \bar{\alpha}^*}{\partial G} = 4.62 \cdot 10^{-3} \left[(\bar{R} + 14.025)^{2.4} \cdot 6.0787 \cdot 10^{-5} + (\bar{G} + 14.025)^{2.4} \cdot 5.271 \cdot 10^{-5} + (\bar{B} + 14.025)^{2.4} \cdot 2.6605 \cdot 10^{-5} \right]^{\frac{2}{3}} (\bar{G} + 14.025)^{1.4} - 9.0848 \cdot 10^{-3} \left[(\bar{R} + 14.025)^{2.4} \cdot 3.1334 \cdot 10^{-5} + (\bar{G} + 14.025)^{2.4} \cdot 1.0542 \cdot 10^{-4} + (\bar{B} + 14.025)^{2.4} \cdot 1.0642 \cdot 10^{-5} \right]^{\frac{2}{3}} (\bar{G} + 14.025)^{1.4} \quad (12)$$

$$\frac{\partial \bar{\alpha}^*}{\partial B} = 2.332 \cdot 10^{-3} \left[(\bar{R} + 14.025)^{2.4} \cdot 6.0787 \cdot 10^{-5} + (\bar{G} + 14.025)^{2.4} \cdot 5.271 \cdot 10^{-5} + (\bar{B} + 14.025)^{2.4} \cdot 2.6605 \cdot 10^{-5} \right]^{\frac{2}{3}} (\bar{B} + 14.025)^{1.4} - 0.9171 \cdot 10^{-3} \left[(\bar{R} + 14.025)^{2.4} \cdot 3.1334 \cdot 10^{-5} + (\bar{G} + 14.025)^{2.4} \cdot 1.0542 \cdot 10^{-4} + (\bar{B} + 14.025)^{2.4} \cdot 1.0642 \cdot 10^{-5} \right]^{\frac{2}{3}} (\bar{B} + 14.025)^{1.4} \quad (13)$$

$$Var(\bar{b}^*) = \left(\frac{\partial \bar{b}^*}{\partial R} \right)^2 VarR + \left(\frac{\partial \bar{b}^*}{\partial G} \right)^2 VarG + \left(\frac{\partial \bar{b}^*}{\partial B} \right)^2 VarB + \left[\frac{\partial \bar{b}^*}{\partial R} \cdot \frac{\partial \bar{b}^*}{\partial G} \cdot Cov(R, G) + \frac{\partial \bar{b}^*}{\partial R} \cdot \frac{\partial \bar{b}^*}{\partial B} \cdot Cov(R, B) + \frac{\partial \bar{b}^*}{\partial G} \cdot \frac{\partial \bar{b}^*}{\partial B} \cdot Cov(G, B) \right] \quad (14)$$

with

$$\frac{\partial \bar{b}^*}{\partial R} = 1.0801 \cdot 10^{-3} \left[(\bar{R} + 14.025)^{2.4} \cdot 3.1334 \cdot 10^{-5} + (\bar{G} + 14.025)^{2.4} \cdot 1.0542 \cdot 10^{-4} + (\bar{B} + 14.025)^{2.4} \cdot 1.0642 \cdot 10^{-5} \right]^{\frac{2}{3}} (\bar{R} + 14.025)^{1.4} - 0.0953 \cdot 10^{-3} \left[(\bar{R} + 14.025)^{2.4} \cdot 2.8448 \cdot 10^{-6} + (\bar{G} + 14.025)^{2.4} \cdot 1.757 \cdot 10^{-5} + (\bar{B} + 14.025)^{2.4} \cdot 1.401 \cdot 10^{-4} \right]^{\frac{2}{3}} (\bar{R} + 14.025)^{1.4} \quad (15)$$

$$\frac{\partial \bar{b}}{\partial \bar{G}} = 3.634 \cdot 10^{-3} \left[(\bar{R} + 14.025)^{2.4} \cdot 3.1334 \cdot 10^{-5} + (\bar{G} + 14.025)^{2.4} \cdot 1.0542 \cdot 10^{-4} + (\bar{B} + 14.025)^{2.4} \cdot 1.0642 \cdot 10^{-5} \right]^{-\frac{2}{3}} (\bar{G} + 14.025)^{1.4} - 0.5887 \cdot 10^{-3} \left[(\bar{R} + 14.025)^{2.4} \cdot 2.8448 \cdot 10^{-6} + (\bar{G} + 14.025)^{2.4} \cdot 1.757 \cdot 10^{-5} + (\bar{B} + 14.025)^{2.4} \cdot 1.401 \cdot 10^{-4} \right]^{-\frac{2}{3}} (\bar{G} + 14.025)^{1.4} \quad (16)$$

$$\frac{\partial \bar{b}}{\partial \bar{B}} = 0.3668 \cdot 10^{-3} \left[(\bar{R} + 14.025)^{2.4} \cdot 3.1334 \cdot 10^{-5} + (\bar{G} + 14.025)^{2.4} \cdot 1.0542 \cdot 10^{-4} + (\bar{B} + 14.025)^{2.4} \cdot 1.0642 \cdot 10^{-5} \right]^{-\frac{2}{3}} (\bar{B} + 14.025)^{1.4} - 4.6943 \cdot 10^{-3} \left[(\bar{R} + 14.025)^{2.4} \cdot 2.8448 \cdot 10^{-6} + (\bar{G} + 14.025)^{2.4} \cdot 1.757 \cdot 10^{-5} + (\bar{B} + 14.025)^{2.4} \cdot 1.401 \cdot 10^{-4} \right]^{-\frac{2}{3}} (\bar{B} + 14.025)^{1.4} \quad (17)$$

V. EXPERIMENTAL RESULTS

We used a number of single-color sRGB images, to compare experimental results to those obtained through equations (6) - (17). Although a single color image appears to a human observer to have only one color shade, its digital equivalent, is composed by many different, though similar, sRGB values, in all three channels of the color-space. First, we statistically compute the values of $\text{Var}(\mathbf{R})$, $\text{Var}(\mathbf{G})$, $\text{Var}(\mathbf{B})$, CovRG , CovRB and CovGB from the original scanned image [8]. Then, we transform this image to the CIEL*a*b* color-space and we computed the values of $\text{Var}(\mathbf{L}^*)$, $\text{Var}(\mathbf{a}^*)$ and $\text{Var}(\mathbf{b}^*)$ [9]. The same values were computed by applying equations (6) - (17) and compared to experimental data. Some indicative results of this study are presented in the next tables.

For a more plausible interpretation of the experimental results, we used the total statistical variances in the two color-spaces.

$$\text{Var}_{sRGB} = \sqrt{\text{Var}_R^2 + \text{Var}_G^2 + \text{Var}_B^2} \quad (18)$$

$$\text{Var}_{L^*a^*b^*} = \sqrt{\text{Var}_{L^*}^2 + \text{Var}_{a^*}^2 + \text{Var}_{b^*}^2}$$

VI. CONCLUSIONS

After a thorough examination of single-color image samples and the extraction of features such as the ones shown in Tables 1, 2 and 3, it emerged that total variances of \mathbf{L}^* , \mathbf{a}^* , \mathbf{b}^* , were always considerably lower than the total variances of \mathbf{R} , \mathbf{G} , \mathbf{B} , ($\text{Var}_{sRGB} > \text{Var}_{L^*a^*b^*}$). The derived mathematical equations for $\text{Var}(\mathbf{L}^*)$, $\text{Var}(\mathbf{a}^*)$ and $\text{Var}(\mathbf{b}^*)$, verify this observation. Its physical meaning is that the transformation $sRGB \rightarrow CIEL^*a^*b^*$ decreases the amount of uncertainty that a digital image carries in the sRGB color-space. This conclusion is quite expectable, taking into account the fact that the human observer perceives single-color images as a single-color shade and that the CIEL*a*b* space is based on the human vision system. It also confirms that, sRGB cannot match the uniformity of CIEL*a*b* space. In our experiments, the difference between Var_{sRGB} and $\text{Var}_{L^*a^*b^*}$ ranges from $\text{Var}_{L^*a^*b^*} = 5\% \text{Var}_{sRGB}$ to $\text{Var}_{L^*a^*b^*} = 25\% \text{Var}_{sRGB}$. Table 4 shows the total variances Var_{sRGB} and $\text{Var}_{L^*a^*b^*}$ of various color samples and the differences between them. These conclusions are reinforced

by results in [10], where it is stated that CIEL*a*b* color-space is the best space for quantization.

Finally, the mathematical formula extracted for the calculation of the \mathbf{L}^* , \mathbf{a}^* , \mathbf{b}^* variances, can be used for designing vision systems, and recognition procedures, to define the limits of uncertainty.

“OLIVE.BMP”					
	Min	Max	Aver.	Statistical Variance	Calculated Variance
\mathbf{L}^*	65.05	67.81	66.2529	0.0796	0.0797
\mathbf{a}^*	14.86	17.86	16.9334	0.7371	0.7370
\mathbf{b}^*	60.68	61.40	61.0771	0.0699	0.1168
\mathbf{R}	210	219	214.964	2.8548	
\mathbf{G}	144	152	147.512	0.7091	
\mathbf{B}	40	47	43.511	0.5155	

Table 1. Statistical results for the color sample ‘olive’.

“WHITE2.BMP”					
	Min	Max	Aver.	Statistical Variance	Calculated Variance
\mathbf{L}^*	99.43	99.9	99.6299	0.0051	0.0064
\mathbf{a}^*	-1.20	0.48	-0.4390	0.0910	0.0705
\mathbf{b}^*	0.714	2.27	1.1259	0.1893	0.1551
\mathbf{R}	253	255	254.040	0.0519	
\mathbf{G}	253	255	254.112	0.1185	
\mathbf{B}	249	252	251.743	0.4605	

Table 2. Statistical results for the color sample ‘white2’.

“YELLOW2.BMP”					
	Min	Max	Aver.	Statistical Variance	Calculated Variance
\mathbf{L}^*	96.44	98.13	97.9350	0.0120	0.0115
\mathbf{a}^*	-19.2	0	-14.894	0.1794	0.1632
\mathbf{b}^*	44.42	57.77	49.730	0.6585	0.6751
\mathbf{R}	243	255	253.881	0.6215	
\mathbf{G}	251	255	254.95	0.1027	
\mathbf{B}	133	160	150.394	3.1380	

Table 3. Statistical results for the color sample ‘yellow2’.

COLOR SAMPLE	Var _{sRGB}	Var _{L*a*b*}	$\frac{Var_{L*a*b*}}{Var_{sRGB}} \%$
red2	0.9905	0.0489	4.93
red1	12.8535	0.6636	5.16
yellow b	6.2454	0.371	5.94
white1	0.0822	0.0057	6.93
white4	8.1353	0.5713	7.02
magenta	11.6943	0.8387	7.17
yellow3	3.0751	0.2291	7.45
yellow1	44.5027	3.4589	7.77
purple1	39.4335	3.2399	8.21
blue1	13.7043	1.1372	8.29
green1	4.211	0.3793	9
gray	1.7705	0.1623	9.16
white2	0.4783	0.0441	9.22
black2	10.3537	0.9627	9.29
yellow4	3.1757	0.3083	9.70
purple2	7.7207	0.8536	11
red3	7.339	0.8272	11.27
black3	15.1929	1.8183	11.96
red4	1.1409	0.1366	11.97
black1	7.2834	0.975	13.38
blue3	8.2933	1.1258	13.57
orange	35.8938	5.0776	14.14
red5	5.6826	0.9005	15.84
blue2	13.4228	2.3659	17.62
green2	15.1174	2.8264	18.69
yellow2	3.2006	0.6826	21.32
olive	2.9863	0.7446	24.93

Table 4. Comparison of the total variances of R, G, B and L*, a*, b* for various color samples.

REFERENCES

- [1] "Processes in biological vision", <http://4colorvision.com/>
- [2] A. N. Venetsanopoulos, K. N. Plataniotis, "Color Image Processing and Applications", Springer 2000.
- [3] "Color Models", <http://www.inforamp.net/~poynton>
- [4] "CIELAB and color wheels", <http://www.handprint.com/HP/WCL/color6.html>
- [5] "Color Calculator – Color-space conversions", <http://www.easyrgb.com/math.html>
- [6] "Color Conversion Algorithms", http://www.cs.rit.edu/~ncs/color/t_convert.html
- [7] "Hewlett-Packard sRGB", <http://www.srgb.com>
- [8] "A Standard Default Color-space for the Internet – sRGB" <http://www.color.org/sRGB.html>
- [9] A.A. Clifford, "Multivariate Error Analysis", Applied Science Publishers Ltd. London
- [10] H. Ikeda, Member, W. Dai and Y. Higaki, "A study on colorimetric errors caused by quantizing color information", *IEEE Transactions on Instrumentation and Measurements*, No.6, 1992, pp. 845-849.